

Article

# In Situ Formation of a Metastable $\beta$ -Ti Alloy by Laser Powder Bed Fusion (L-PBF) of Vanadium and Iron Modified Ti-6Al-4V

Florian Huber <sup>1,2,3,\*</sup>, Thomas Papke <sup>3,4</sup>, Christian Scheitler <sup>1,2,3</sup>, Lukas Hanrieder <sup>1</sup>, Marion Merklein <sup>3,4</sup> and Michael Schmidt <sup>1,2,3</sup>

<sup>1</sup> Institute of Photonic Technologies, Friedrich-Alexander-University Erlangen-Nürnberg (FAU), Konrad-Zuse-Straße 3/5, 91052 Erlangen, Germany; sekretariat@lpt.uni-erlangen.de (C.S. & L.H. & M.S.)

<sup>2</sup> Erlangen Graduate School in Advanced Optical Technologies (SAOT), Paul-Gordan-Straße 6, 91052 Erlangen, Germany

<sup>3</sup> Collaborative Research Center 814—Additive Manufacturing, Am Weichselgarten 8, 91058 Erlangen, Germany; thomas.papke@fau.de (T.P.); sabine.wittmann@fau.de (M.M.)

<sup>4</sup> Institute of Manufacturing Technology, Friedrich-Alexander-University Erlangen-Nürnberg (FAU), Egerlandstraße 11–13, 91058 Erlangen, Germany

\* Correspondence: florian.huber@lpt.uni-erlangen.de; Tel.: +49-09131-85-23241

Received: 27 November 2018; Accepted: 13 December 2018; Published: 14 December 2018



**Abstract:** The aim of this work is to investigate the  $\beta$ -Ti-phase-stabilizing effect of vanadium and iron added to Ti-6Al-4V powder by means of heterogeneous powder mixtures and in situ alloy-formation during laser powder bed fusion (L-PBF). The resulting microstructure was analyzed by metallographic methods, scanning electron microscopy (SEM), and electron backscatter diffraction (EBSD). The mechanical properties were characterized by compression tests, both prior to and after heat-treating. Energy dispersive X-ray spectroscopy showed a homogeneous element distribution, proving the feasibility of in situ alloying by LPBF. Due to the  $\beta$ -phase-stabilizing effect of V and Fe added to Ti-6Al-4V, instead of an  $\alpha'$ -martensitic microstructure, an  $\alpha/\beta$ -microstructure containing at least 63.8%  $\beta$ -phase develops. Depending on the post L-PBF heat-treatment, either an increased upsetting at failure (33.9%) compared to unmodified Ti-6Al-4V (28.8%), or an exceptional high compressive yield strength ( $1857 \pm 35$  MPa compared to 1100 MPa) were measured. The hardness of the in situ alloyed material ranges from  $336 \pm 7$  HV0.5, in as-built condition, to  $543 \pm 13$  HV0.5 after precipitation-hardening. Hence, the range of achievable mechanical properties in dependence of the post-L-PBF heat-treatment can be significantly expanded in comparison to unmodified Ti-6Al-4V, thus providing increased flexibility for additive manufacturing of titanium parts.

**Keywords:** laser powder bed fusion (L-PBF); additive manufacturing; titanium alloys; microstructure; compression test

## 1. Introduction

Laser powder bed fusion (L-PBF), also referred to as selective laser melting (SLM) or laser beam melting (LBM), is currently the most widely used technique for additive manufacturing of metals [1]. Figure 1 shows a basic schematic of the process. Especially for demanding applications, e.g., in the aerospace industry [2] or for medical implants [3] titanium alloys are of particular interest. The most important titanium alloy for L-PBF applications is Ti-6Al-4V [4]. L-PBF of Ti-6Al-4V is, in general, well understood and standard parameter sets are available for numerous commercial L-PBF systems (e.g., EOS M 290 [5] or SLM 280 [6]). Recent scientific publications focus, for example, on the microstructure evolution [7] or the fatigue behavior [8] of Ti-6Al-4V processed by L-PBF. However,

the usage of alternative titanium alloys for L-PBF is rather uncommon. Reasons for this are an elaborate development of process parameters for new alloys and the limited availability of suitable pre-alloyed powders as starting material for L-PBF. The atomization of special alloys on demand is possible, but generally linked with high costs. One approach for developing new Ti alloys for L-PBF is in situ alloying from heterogeneous powder mixtures made from commercially available standard powders. Aiming for an increased wear resistance, Gu [9] reported a similar approach for producing metal matrix composites. For this purpose, SiC and commercially pure Ti powder were blended using a ball mill. After L-PBF, the resulting parts showed an elevated microhardness (>980 HV0.3) and wear resistance in comparison to pure Ti. With respect to antibacterial properties, Macpherson et al. [10] published a study on adding Cu and Ag to Ti-6Al-4V by in situ alloying. Energy dispersive X-ray spectroscopy (EDS) measurements showed a homogeneous distribution of the added elements after L-PBF. Also motivated by medical applications, Sing et al. [11] investigated in situ alloying of Ti with 50 wt % Ta, and showed that a microstructure predominantly consisting of  $\beta$ -phase evolved. However, no heat-treatments were performed to adjust the mechanical properties and to remove the internal stress induced during L-PBF, and the homogeneity of the element distribution after L-PBF was partly not investigated. Furthermore, with respect to load-bearing applications, e.g., in the aerospace industry, alloy compositions different than those described in the abovementioned works, are required. Due to their exceptional mechanical properties and, especially, their high cycle fatigue strength, metastable  $\beta$ -Ti alloys, like Ti-10V-2Fe-3Al, are becoming increasingly important for aircraft parts [12]. Thus, aim of this work is to investigate the modification of Ti-6Al-4V with the  $\beta$ -phase-stabilizing elements, V and Fe, by means of heterogeneous powder mixtures and in situ alloying during L-PBF. Following L-PBF, different heat-treatments were conceived and applied to the in situ alloyed samples. Subsequently, the resulting element distribution, as a criterion for a successful in situ alloy formation, as well as the microstructure and the mechanical properties, were analyzed.

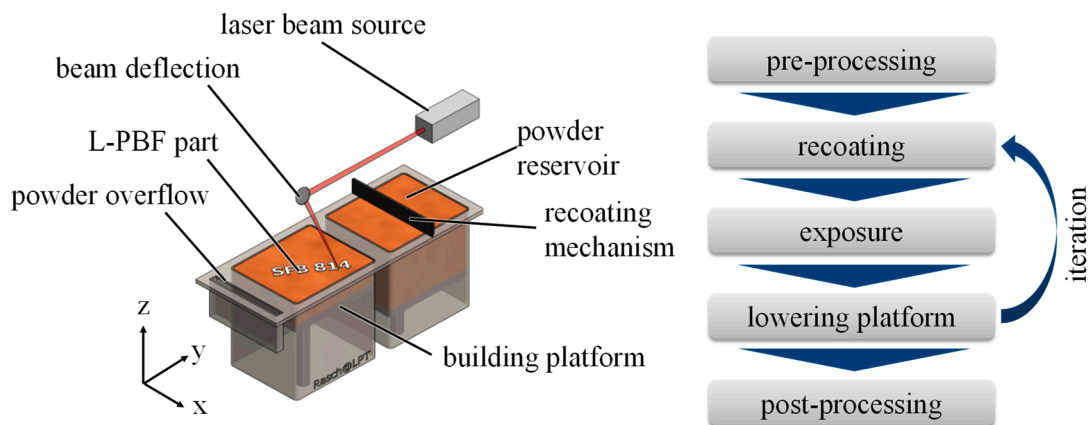


Figure 1. Schematic of the L-PBF process.

## 2. Materials and Methods

The predominantly spherical Ti-6Al-4V with a particle size distribution of 15–45  $\mu\text{m}$ , used in this work, was obtained from AP&C Advanced Powders and Coatings Inc. (Boisbriand, QC, Canada). The irregular-shaped V and Fe powders, also with a nominal particle size distribution of <45  $\mu\text{m}$ , were provided by PMCtec GmbH (Leun Germany) and NMD GmbH (Heemsen, Germany), respectively. The chemical composition of the powders was analyzed by EDS and are listed in Table 1. Figure 2 shows scanning electron images (SEM) of the powders. For the L-PBF experiments, the Ti-6Al-4V powder was blended with commercially pure Fe and V powder (ratio: 91.67 Ti-6Al-4V/2.00 Fe/6.33 V). The mixing procedure was experimentally developed and comprises vibration sieving to break up potential agglomerates, and subsequent mixing for two hours in a Turbula<sup>®</sup>-mixer from Willy A. Bachofen AG (Muttentz, Switzerland). The intention was to achieve a relative element

distribution throughout the heterogeneous powder mixture close to the commercial metastable  $\beta$ -alloy Ti-10V-2Fe-3Al. Since an exact Al concentration of the target alloy is not achievable by adding Fe and V to Ti-6Al-4V powder, the resulting nominal elemental distribution is 82.5 Ti/10 V/2 Fe/5.5 Al and, therefore, shows a slightly higher aluminum content than the target alloy. Despite the non-spherical particle shape of the Fe and V powders, the powder system obtained from the mixing procedure can be recoated to homogeneous layers without significant imperfections. This was verified visually by an illumination setup and a high-resolution camera.

**Table 1.** Chemical composition of the powder batches used in this study determined by EDS analysis.

Material	Ti	Al	V	Fe	Si
Specification					
Ti-6Al-4V (wt %) [13]	bal.	5.5–6.75	3.5–4.5	0.0–0.3	-
Ti-6Al-4V (wt %)	89.3	6.3	4.2	0.2	-
Fe (wt %)	-	-	-	99.8	0.1
V (wt %)	-	-	99.9	-	-
standard deviation < 0.1 wt %					

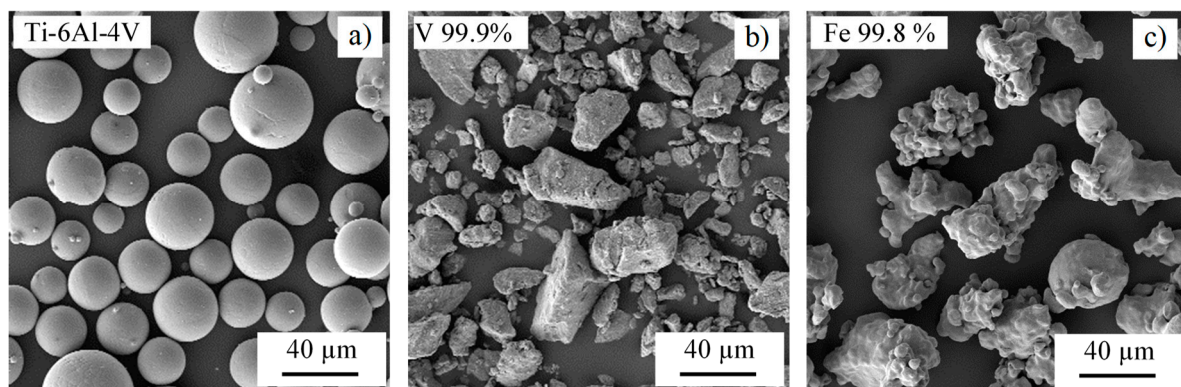


**Figure 2.** SEM images of the powders used in this work: (a) Ti-6Al-4V powder, (b) V powder, (c) Fe powder.

To analyze the effect of the addition of V and Fe to Ti-6Al-4V by in situ alloying on the microstructure and the mechanical properties, 30 cylindrical samples with the dimensions  $\varnothing$  7.5 mm  $\times$  19 mm were manufactured using a SLM 50 L-PBF-machine from Realizer GmbH (Borchen, Germany). Eighteen samples were built with Ti-6Al-4V powder modified with V and Fe, while 12 samples have been built with non-modified Ti-6Al-4V powder as reference group. The parameter sets used for manufacturing the specimens are listed in Table 2. The parameters were experimentally developed and facilitate the production of parts with relative densities above 99.9%. For each powder material, the parameter set facilitating the highest relative densities was selected from a series of 36 test samples, that were built with varying scan speeds (300, 600, and 900 mm/s), spot diameters (40 and 70  $\mu$ m), and hatch distances (60, 90, and 120  $\mu$ m). The highest relative densities for the Ti-6Al-4V + 2Fe + 6V powder mixture are achievable with a reduced spot diameter compared to unmodified Ti-6Al-4V. This is probably due to the altered chemical composition.

**Table 2.** Parameter sets used for manufacturing the samples.

Material	Laser Power	Scan Speed	Spot Diameter	Hatch Distance	Layer Thickness
Ti-6Al-4V	100 W	600 mm/s	70 $\mu$ m	60 $\mu$ m	30 $\mu$ m
Ti-6Al-4V + 2Fe + 6V	100 W	600 mm/s	40 $\mu$ m	60 $\mu$ m	30 $\mu$ m

Following the L-PBF process, a group of six samples of each material was heat-treated at 850 °C for two hours, and cooled in the furnace. This heat-treatment, which was developed for Ti-6Al-4V from L-PBF, was derived from Vrancken et al. [14], and also applied in previous work [15]. All heat-treatments were performed in a furnace constantly flushed with argon to reduce oxidation and oxygen absorption. Furthermore, an additional heat-treatment for a group of six Ti-6Al-4V + 2Fe + 6V samples was conceived. It comprised a solution heat-treatment at 1050 °C (above  $\beta$ -transus temperature) for 20 min, followed by water quenching and annealing at 500 °C for eight hours. These values were partially derived from [12]. The intention of this heat-treatment is to dissolve the microstructure developed during L-PBF by the occurring phase transition related to the temperatures above  $\beta$ -transus temperature, and the subsequent water quenching. For achieving a strengthening effect, the homogeneous precipitation of fine dispersed  $\alpha$ -phase within the  $\beta$ -phase matrix by the annealing at 500 °C is proposed. The heat-treatments used in this work are summed up in Table 3. The S 1050 °C + PH heat-treatment was not applied to the unmodified Ti-6Al-4V reference samples, since, without the presumed  $\beta$ -phase-stabilizing effect of the Fe and V addition, the formation of  $\alpha'$ -martensite, instead of  $\beta$ -phase, that would be required for the precipitation-hardening after water quenching, is to be expected.

**Table 3.** Heat-treatments applied to the specimens.

AN 850 °C	Annealed at 850 °C, 2 h
S 1050 °C + PH	Solution heat-treated at 1050 °C, 20 min; water quenched; precipitation-hardened at 500 °C, 8 h

The resulting microstructure in dependence of the alloy composition and the heat-treatment condition was characterized by analyzing metallographically prepared cross-sections by means of EDS, scanning electron imaging (SEM), and electron backscatter diffraction (EDSB). For this purpose, the specimens were grinded and polished with 3  $\mu$ m diamond suspension, followed by a polishing step with active oxide polishing suspension (OPS) and hydrogen peroxide. To reveal the microstructure, the samples were cleaned in an ultrasonic bath and etched with Kroll's reagent (H<sub>2</sub>O, HNO<sub>3</sub>, HF) for 8 s and investigated by optical microscopy. The mechanical properties were characterized by compression tests and hardness measurements. The microhardness was measured using a KB 30 S device from Hegewald & Peschke Meß- und Prüftechnik GmbH (Nossen, Germany). For determining the compression properties, five samples of each group have been processed to specimens with the dimensions  $\varnothing$  6 mm  $\times$  9 mm by successive turn-milling and grinding. Further information on the experimental setup is given in prior work [16]. The tests were performed in accordance with DIN 50106 [17].

### 3. Results and Discussion

One criterion for the success of the in situ alloying approach, by means of heterogeneous powder mixtures and L-PBF, is to accomplish the desired elemental distribution homogeneously throughout the L-PBF part. This was investigated by EDS. As shown in Figure 3, after annealing at 850 °C, only minor inhomogeneity is visible, and the elements are evenly distributed across the part. The original powder particles with a size of 1 to 45  $\mu$ m are completely fused and mixed, and no unmelted areas consisting of pure V, Fe, or Ti-6Al-4V are visible. A significant demixing effect of the powder particles during powder handling or recoating was not observed, as the element concentration in the resulting parts was found to be homogeneous. The resulting alloying element concentration was determined to be  $81.9 \pm 0.06$  wt % titanium,  $10.8 \pm 0.05$  wt % vanadium,  $2.0 \pm 0.03$  wt % iron, and  $5.2 \pm 0.06$  wt % aluminum, and is therefore close to the expected 82.5 Ti/10 V/2 Fe/5.5 Al composition. The slightly lower amount of aluminum, in comparison to the calculated value of 5.5 wt %, presumably originates from aluminum evaporation during L-PBF, that was also observed in previous work [18]. The EDS results demonstrate the general feasibility of in situ alloying for developing new Ti alloys for L-PBF applications.

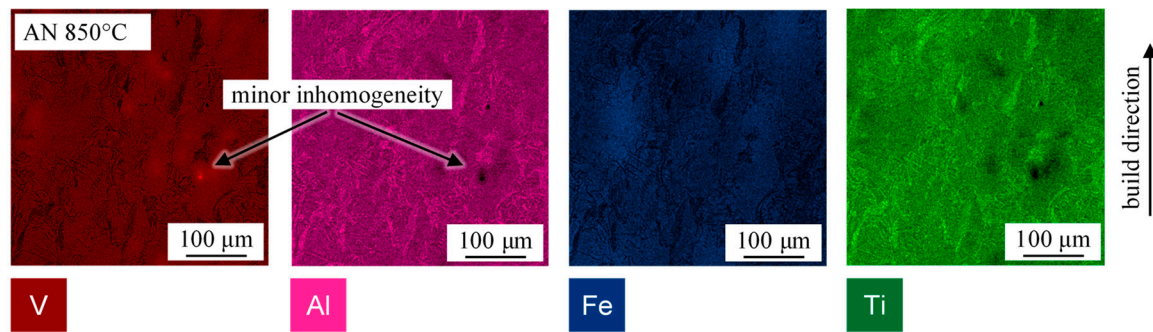


**Figure 3.** EDS analysis of the in situ alloyed Ti-6Al-4V + 2Fe + 6V material; from left to right: elemental mapping for the elements V, Al, Fe, and Ti.

The resulting microstructure in dependence of the alloy composition and the heat-treatment is shown in Figure 4. In as-built condition, the Ti-6Al-4V reference samples consist of an  $\alpha'$ -martensitic microstructure with elongated, columnar prior  $\beta$ -grains, and a hardness of  $424 \pm 11$  HV0.5. The  $\alpha'$ -martensite is formed due to the high cooling rates in the range of 106 K/s [19], that are related to the L-PBF process. This is well in accordance with literature (e.g., [20]). A heat-treatment at 850 °C leads to a decomposition of the  $\alpha'$ -martensite into fine acicular  $\alpha$ -phase surrounded by  $\beta$ -phase, while the prior  $\beta$ -grains remain visible, since the  $\beta$ -transus temperature of Ti-6Al-4V at around 960 °C [12] is not exceeded. The hardness is reduced to  $364 \pm 14$  HV0.5, due to the change in microstructure. The amount of  $\beta$ -phase was determined to be 15% by EBSD measurements.

V and Fe addition to Ti-6Al-4V, by means of in situ alloying, results in a significant change in the microstructure compared to unmodified Ti-6Al-4V reference samples. No  $\alpha'$ -martensite is formed during L-PBF of the in situ alloyed samples, and the hardness is with  $336 \pm 7$  HV0.5, significantly lower than the hardness of the unmodified alloy in as-built condition, with  $424 \pm 11$  HV0.5. Instead, a microstructure consisting of intertwined  $\alpha$ - and  $\beta$ -grains evolves (Figures 4 and 5). EBSD measurements show the presence of at least 63.8%  $\beta$ -phase and 26.6%  $\alpha$ -phase (9.6% unresolved areas, presumed to be predominantly  $\alpha$ -phase) in as-built condition. The  $\beta$ -phase-stabilizing effect of the elements V and Fe [12] can, therefore, be confirmed for the L-PBF process.

Heat-treatment of the Ti-6Al-4V + 2Fe + 6V samples at 850 °C results in cellular  $\beta$ -grains with  $\alpha$ -phase located at the grain boundaries and acicular  $\alpha$ -phase platelets inside the  $\beta$ -grains (Figures 4 and 5). Due to the microstructural changes, it is assumed that a complete phase transition takes place during the 850 °C heat-treatment, and the as-built microstructure is dissolved. This indicates that the  $\beta$ -transus temperature of the in situ alloyed material is reduced below 850 °C by the  $\beta$ -phase-stabilizing effect the alloying elements V and Fe (see also  $\beta$ -transus temperature of the commercial alloy Ti-10V-2Fe-3Al at 800 °C [21]). During the subsequent cooling, from 850 °C to room temperature in the furnace, a more equilibrium material state evolves than during the L-PBF process, that comprises cooling rates in the range of 106 K/s [19]. Due to the lower cooling rates, slightly less  $\beta$ -phase with a share of 57.8% is obtained after the 850 °C heat-treatment, than directly after L-PBF. Solution heat-treatment at 1050 °C, and subsequent water quenching and precipitation heat-treatment leads, as intended, to very fine, homogeneously distributed nm-scale  $\alpha$ -precipitations inside cellular  $\beta$ -grains (Figures 4 and 5). The very high hardness of  $534 \pm 13$  HV0.5, measured for the sample, presumably originates from these precipitations, and indicates a high mechanical strength.

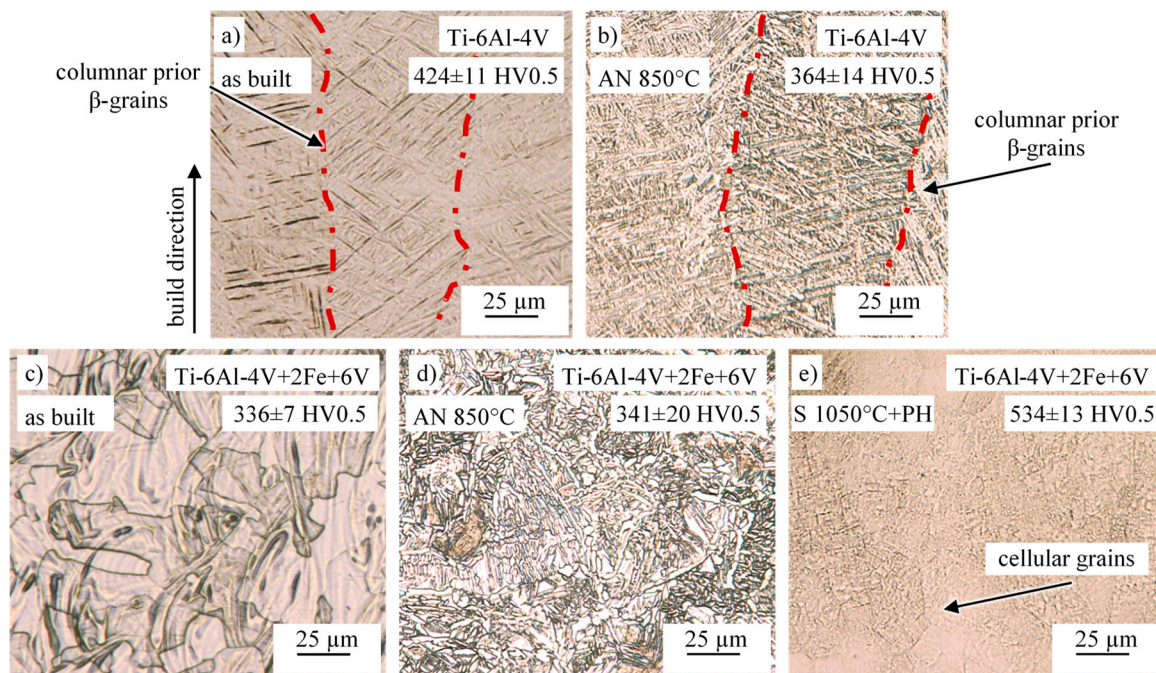


**Figure 4.** Resulting microstructure and microhardness ( $n = 8$ ) in dependence of the alloy composition and the heat-treatment (oxide polishing suspension (OPS)-polished and etched with Kroll's reagent): (a) Ti-6Al-4V as-built, (b) Ti-6Al-4V heat-treated at 850 °C, (c) Ti-6Al-4V + 2Fe + 6V as-built, (d) Ti-6Al-4V + 2Fe + 6V heat-treated at 850 °C, (e) Ti-6Al-4V + 2Fe + 6V solution heat-treated at 1050 °C and precipitation-hardened.

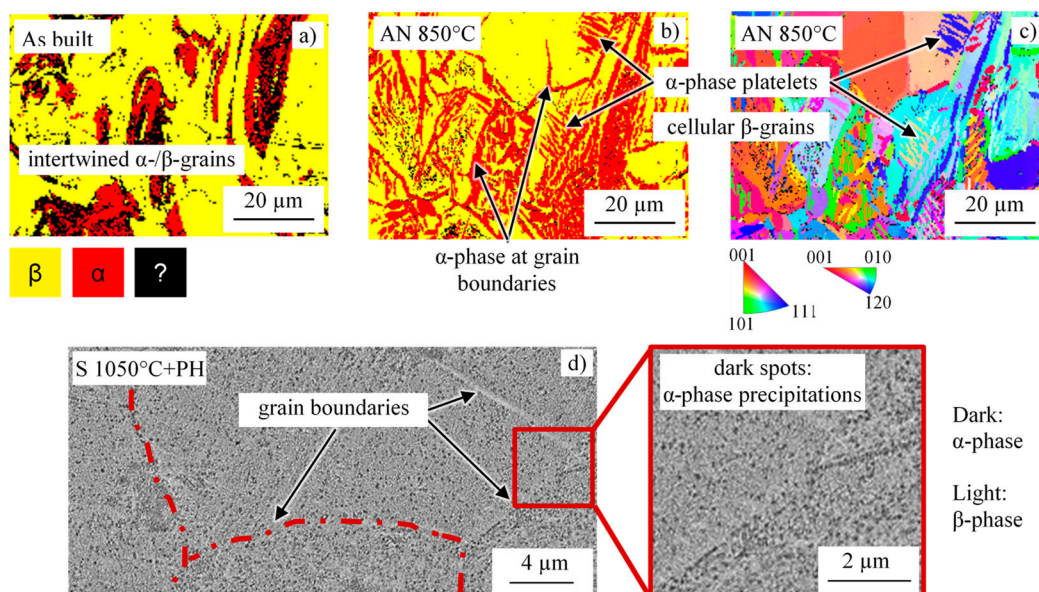


**Figure 5.** (a,b): EBSD phase-mapping, (c): EBSD inverse pole figure (ipf) map corresponding to (b,d): SEM images of the in situ alloyed Ti-6Al-4V + 2Fe + 6V samples.

The effect of in situ alloying and the heat-treatments on the mechanical properties of the material was investigated by compression tests. The resulting mean compressive yield stresses ( $\sigma_{d0.2}$ ) out of five samples, which are evaluated at a plastic upsetting of 0.2%, are shown in Figure 6 (left). Furthermore,  $\epsilon_{dtM, \min}$ , representing the minimal upsetting at failure measured in each group of five samples, is plotted in Figure 6 (right). The failure is characterized by the break of the specimen under pressure load. In as-built condition, the Ti-6Al-4V + 2Fe + 6V material reaches a slightly lower yield strength

than the Ti-6Al-4V reference group, but the minimal upsetting at failure increases from 17.2% to 25.2% as a consequence of the in situ alloying. The 850 °C heat-treatment increases the minimal upsetting at failure for pure Ti-6Al-4V, as well as for the modified alloy, due to microstructural changes shown in Figures 4 and 5. The in situ alloyed and 850 °C heat-treated samples again show a higher upsetting at break of 33.9% compared to 25.2% of the Ti-6Al-4V reference group. This behavior can be explained by the increased amount of  $\beta$ -phase (from 15% to 58%) resulting from in situ alloying with the  $\beta$ -phase-stabilizing elements V and Fe (Figure 5). The  $\beta$ -phase provides a higher amount of slip planes due to its body-centered cubic (bcc) structure in comparison to the hexagonal close-packed (hcp) structure of the  $\alpha$ -phase [12] and, therefore, the ductility and, hence, the upsetting at fracture increases.

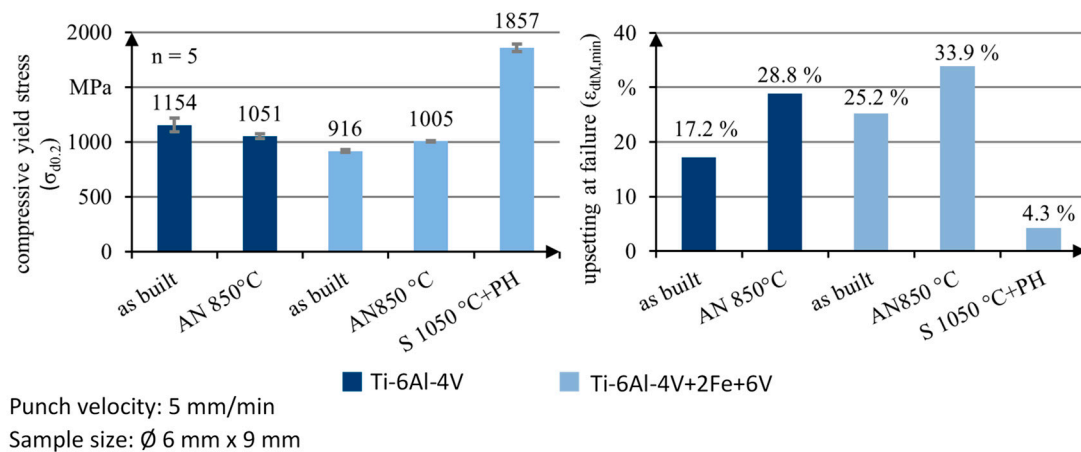


**Figure 6.** Compressive yield stress and minimal upsetting at failure out of five samples in dependence of the alloy composition and the heat-treatment. (Left): compressive yield stress; (right): upsetting at failure.

In contrast to that, the 1050 °C heat-treatment results in an exceptional high compressive yield stress of  $1857 \pm 35$  MPa for the in situ alloyed Ti-6Al-4V + 2Fe + 6V samples. This value significantly surpasses Ti-6Al-4V and, also, the commercial alloy Ti-10V-2Fe-3Al at a similar heat-treatment state with a compressive yield stress of 1145 MPa [21]. This is probably related to the strengthening effect of the nm-scale  $\alpha$ -precipitations observed in Figure 5. A possible explanation for the higher compressive yield stress in comparison to Ti-10V-2Fe-3Al is the  $\alpha$ -phase-stabilizing effect of the higher amount of aluminum of the in situ alloyed Ti-6Al-4V + 2Fe + 6V material. Additionally, oxygen, that might have been taken up during L-PBF, could act as  $\alpha$ -phase stabilizer. This could possibly lead to an increased amount of  $\alpha$ -phase precipitations compared to forged and heat-treated commercial Ti-10V-2Fe-3Al, and might explain the elevated compressive yield stress. However, the upsetting at fracture of the 1050 °C heat-treated Ti-6Al-4V + 2Fe + 6V shows a comparable low value of 4.3%, which is significantly below the values measured for Ti-6Al-4V, but is in good agreement with an elongation at break of 4.0% specified for the commercial alloy Ti-10V-2Fe-3Al with a similar heat-treatment state [21]. As a result of the modification of Ti-6Al-4V with V and Fe, the range of achievable mechanical properties in dependence of the heat-treatment is significantly expanded.

#### 4. Conclusions

In summary, this publication describes the modification of Ti-6Al-4V with the  $\beta$ -phase-stabilizing elements V and Fe by means of heterogeneous powder mixing and in situ alloying during L-PBF. The  $\beta$ -phase-stabilizing effect of the elements Fe and V, and the general feasibility of in situ alloying for the swift development of new alloys for L-PBF-applications, are confirmed. The results demonstrate the possibility of obtaining a metastable  $\beta$ -Ti alloy close to the commercial alloy Ti-10V-2Fe-3Al from Ti-6Al-4V, V, and Fe powder without the need for expensive atomization of customized pre-alloyed powder. EBSD analysis shows a  $\beta$ -phase content of at least 63.8% in as-built condition, whereas

unmodified Ti-6Al-4V develops an  $\alpha'$ -martensitic microstructure. In dependence of the post-L-PBF heat-treatment either an increased minimum upsetting at failure of 33.9%, in comparison to 28.8% for unmodified Ti-6Al-4V, or an exceptional high compressive yield strength of  $1857 \pm 35$  MPa in comparison to about 1100 MPa for unmodified Ti-6Al-4V, can be achieved. The hardness of the in situ alloyed material ranges from  $336 \pm 7$  HV0.5, in as-built condition, to  $543 \pm 13$  HV0.5 after precipitation-hardening. Modification of Ti-6Al-4V with Fe and V consequently expands the range of mechanical properties that can be achieved in dependence of the heat-treatment. This provides additional flexibility for developing sophisticated titanium parts with tailored material properties.

**Author Contributions:** F.H. wrote the paper. F.H. developed the methodology and designed the experiments. F.H. performed the experiments together with L.H. T.P. performed the compression test and provided his expertise regarding the interpretation of the same. C.S. contributed additional expertise regarding the discussion of the results and the preparation of the manuscript. M.M. and M.S. supervised the work.

**Funding:** This research was funded by the German Research Foundation (DFG), Germany [Collaborative Research Center 814: Additive Manufacturing, Subproject B5; Erlangen Graduate School in Advanced Optical Technologies (SAOT)].

**Acknowledgments:** We acknowledge support by the German Research Foundation (DFG) and Friedrich-Alexander-Universität Erlangen-Nürnberg (FAU) within the funding program Open Access Publishing.

**Conflicts of Interest:** The authors declare no conflict of interest.

## References

1. Wohlers, T.; Caffrey, T.; Campbell, I. *Wohlers Report 2016 Published*; Wohlers Associates, Inc.: Fort Collins, CO, USA, 2016; ISBN 9780991333226.
2. Uhlmann, E.; Kersting, R.; Klein, T.B.; Cruz, M.F.; Borille, A.V. Additive manufacturing of titanium alloy for aircraft components. *Procedia CIRP* **2015**, *35*, 55–60. [[CrossRef](#)]
3. Rotaru, H.; Schumacher, R.; Kim, S.-G.; Dinu, C. Selective laser melted titanium implants: a new technique for the reconstruction of extensive zygomatic complex defects. *Maxillofac. Plast. Reconstr. Surg.* **2015**, *37*, 12. [[CrossRef](#)]
4. Dutta, B.; Froes, F.H. *Additive manufacturing of Titanium Alloys: State of the Art, Challenges and Opportunities*; Butterworth-Heinemann: Oxford, UK, 2015; ISBN 9780128047828.
5. EOS GmbH No Title. Available online: <https://www.eos.info/material-m> (accessed on 10 September 2018).
6. SLM Solutions GmbH No Title. Available online: <https://slm-solutions.com/products/accessories-and-consumables/slmr-metal-powder> (accessed on 11 September 2018).
7. Zhai, Y.; Galarraga, H.; Lados, D.A. Microstructure evolution, tensile properties, and fatigue damage mechanisms in Ti-6Al-4V alloys fabricated by two additive manufacturing techniques. *Procedia Eng.* **2015**, *114*, 658–666. [[CrossRef](#)]
8. Chastand, V.; Tezenas, A.; Cadoret, Y.; Quaegebeur, P.; Maia, W.; Charkaluk, E. Fatigue characterization of Titanium Ti-6Al-4V samples produced by additive manufacturing. *Procedia Struct. Integr.* **2016**, *2*, 3168–3176. [[CrossRef](#)]
9. Gu, D. *Laser Additive Manufacturing of High-Performance Materials*; Springer: Heidelberg, Germany, 2015.
10. Macpherson, A.; Li, X.; McCormick, P.; Ren, L.; Yang, K.; Sercombe, T.B. Antibacterial titanium produced using selective laser melting. *JOM* **2017**, *69*, 2719–2724. [[CrossRef](#)]
11. Sing, S.L.; Yeong, W.Y.; Wiria, F.E. Selective laser melting of titanium alloy with 50 wt% tantalum: Microstructure and mechanical properties. *J. Alloys Compd.* **2016**, *660*, 461–470. [[CrossRef](#)]
12. Leyens, C.; Peters, M. *Titanium and Titanium Alloys: Fundamentals and Applications*; John Wiley & Sons: Hoboken, NJ, USA, 2003; ISBN 3527305343.
13. DIN 17851. *Titanium Alloys; Chemical Composition*; Deutsches Institut für Normung E.V. (DIN): Berlin, Germany, 1990.
14. Vrancken, B.; Thijs, L.; Kruth, J.P.; Van Humbeeck, J. Heat treatment of Ti6Al4V produced by selective laser melting: microstructure and mechanical properties. *J. Alloys Compd.* **2012**, *541*, 177–185. [[CrossRef](#)]
15. Butzhammer, L.; Dubjella, P.; Huber, F.; Schaub, A.; Aumüller, M.; Petrunenko, O.; Merklein, M.; Schmidt, M. Experimental Investigation of a Process Chain Combining Sheet Metal Bending and Laser Beam Melting of Ti-6Al-4V. In Proceedings of the Lasers in Manufacturing Conference, Munich, Germany, 26–29 June 2017.

16. Papke, T.; Junker, D.; Schmidt, M.; Kolb, T.; Merklein, M. Bulk Metal Forming of Additively Manufactured Elements. In Proceedings of the 5th International Conference on New Forming Technology, Bremen, Germany, 18–21 September 2018.
17. DIN 50106. *Testing of Metallic Components—Compression Test at Room Temperature*; Deutsches Institut für Normung E.V. (DIN): Berlin, Germany, 2016.
18. Huber, F.; Rasch, M.; Butzhammer, L.; Karg, M.; Schmidt, M. Strahlschmelzen von Metallen mit unterschiedlichen Intensitäten und Belichtungsstrategien. In Proceedings of the 5. Industriekolloquium des Sonderforschungsbereichs 814—Additive Fertigung, Nürnberg, Germany, 12 December 2017.
19. Mukherjee, T.; Wei, H.L.; De, A.; DebRoy, T. Heat and fluid flow in additive manufacturing—Part II: Powder bed fusion of stainless steel, and titanium, nickel and aluminum base alloys. *Comput. Mater. Sci.* **2018**, *150*, 369–380. [[CrossRef](#)]
20. Xu, W.; Brandt, M.; Sun, S.; Elambasseril, J.; Liu, Q.; Latham, K.; Xia, K.; Qian, M. Additive manufacturing of strong and ductile Ti-6Al-4V by selective laser melting via in situ martensite decomposition. *Acta Mater.* **2015**, *85*, 74–84. [[CrossRef](#)]
21. Titanium Metals Corporation Timetal® 10-2-3. Available online: <http://www.timet.com/assets/local/documents/datasheets/metastablebetaalloys/10-2-3.pdf> (accessed on 11 September 2018).



© 2018 by the authors. Licensee MDPI, Basel, Switzerland. This article is an open access article distributed under the terms and conditions of the Creative Commons Attribution (CC BY) license (<http://creativecommons.org/licenses/by/4.0/>).